Defect-related visible luminescence of ZnO nanorods annealed in oxygen ambient*

CAI Jing-wei(蔡井维)[1], **XU Jian-ping**(徐建萍)[1], **ZHANG Xiao-song**(张晓松)[1], **NIU Xi-ping**(牛喜平)[1], **XING Tong-yan**(邢彤焱)[1], **JI Ting**(季婷)[2], **and LI Lan**(李岚)[1]**

1. Key Laboratory of Display Materials and Photoelectric Devices of Education Ministry of China, Key Laboratory for Optoelectronic Materials and Devices, Insitute of Material Physics, Tianjin University of Technology, Tianjin 300384, China

2. Tianjin Xinhua Staff and Workers University, Tianjin 300040, China

(Received 7 June 2011)

ZnO nanorods prepared by a solution-phase method are annealed at different temperatures in oxygen ambient. The luminescence properties of the samples are investigated. In the same excitation condition, the photoluminescence (PL) spectra of all samples show an ultraviolet (UV) emission and a broad strong visible emission band. The asymmetric visible emission band of annealed samples has a red-shift as the annealing temperature increasing from 200 °C to 600 °C and it can be deconvoluted into two subband emissions centered at 535 nm (green emission) and 611 nm (orange-red emission) by Gaussian-fitting analysis. Analyses of PL excitation (PLE) spectra and PL spectra at different excitation wavelengths reveal that the green emission and the orange-red emission have a uniform initial state, which can be attributed to the electron transition from Zn interstitial (Zn_i) to oxygen vacancy (V_o) and oxygen interstitial (O_i), respectively.

Document code: A **Article ID:** 1673-1905(2012)01-0004-5

DOI 10.1007/s11801-012-1042-2

As a wide bandgap semiconductor with the large exciton binding energy at room temperature, ZnO has received wide attention due to its important applications in gas sensors, solar cells, thin-film transistors and light emitting diodes (LEDs)[1,2]. ZnO nanostructures typically exhibit ultraviolet (UV) and visible emission bands. The UV emission is commonly considered as the near band-edge emission or the exciton recombination emtssion[3-5], and the visible emission bands are generally attributed to the extrinsic or intrinsic defects in ZnO, such as intended dopants, oxygen vacancy (V_o), Zn interstitial (Zn_i), oxygen interstitial (O_i) and so on[6,7]. The formation of the defects in ZnO nanostructures is closely related to the preparation conditions and postannealing temperature and ambient, which can influence the properties of ZnO based devices[8-13]. After annealed in oxygen ambient, the defect emission around 510 nm of ZnO nanowires prepared by chemical vapor deposition (CVD) is passivated and an electroluminescence device peaked at 382 nm is obtained[8]. In ZnO nanoparticles based thin-film transistor device, the decrease of V_o defects in ZnO nanoparticles enhances the field-effect mobility and lowers the threshold voltage[9]. Intended suppression of the intrinsic defects in ZnO nanorods significantly increases open circuit voltage (V_{oc}) and reduces the charge recombination rate in poly(2-methoxy, 5-(2'-ethylhexyloxy)-1, 4-phenylenevinylene and ZnO (MEH-PPV/ZnO) hybrid photovoltaic devices[10,11]. The formation of V_o defects in ZnO nanowire is found to accelerate the response time and recovery sensitivity in NO_2 gas sensor[12]. The combination of intense defect-related green-yellow emission from ZnO nanorods with the blue emission from polyfluorene can achieve white light emission under applied electric field[13]. However, the origins of defect-related emission in the visible region are still in controversial discussion. For example, green emission is typically attributed to V_o defets, Zn_i defects[14], surface states as well as Cu impurities[15,16], whereas yellow emission, which is commonly observed in ZnO

* This work has been supported by the National Natural Science Foundation of China (Nos.60877029, 10904109, 60977035 and 60907021), the Natural Science Foundation of Tianjin (Nos.09JCYBJC01400 and 10SYSYJC28100), the Key Subject for Materials Physics and Chemistry of Tianjin, and the Open Foundation of Key Laboratory of Luminescence and Optical Information of Ministry of Education (Nos.2010LOI02 and 2010LOI11).

** E-mail: lilan@tjut.edu.cn

nanostructures prepared by aqueous solution method, is attributed to Zn_i defects, O_i defects, $Zn(OH)_2$ and Li impurities[17]. It is essential to identify the origins of the defect-related emissions and investigate the electron transition processes.

In this letter, ZnO nanorods are fabricated by a low temperature solution-phase method, which is annealed in oxygen ambient at different temperatures. PLE and PL spectra are used to investigate the possible origins of defect-related emissions and observe the processes of photogenerated charge carrier transfer and recombination in ZnO nanorods.

ZnO nanorods are prepared from an aqueous mixture solution of zinc nitrate hexahydrate (0.1 M) and methenamine (0.1 M). Two precursor solutions are transferred into a reaction beaker and stirred for 30 min, and then SiO_2-coated Si substrate is vertically immersed into the solution. After heated at 95 °C for 4 h in sealed container, a white layer of the product is deposited on the substrate. The products are washed by deionized water for several times, and then annealed in oxygen ambient at 200 °C, 400 °C, 500 °C and 600 °C, respectively.

The morphology of the product is analyzed by scanning electron microscopy (SEM, JSM-6700F). X-ray diffraction (XRD) patterns are examined by a Rigaku 2500/PC X-ray diffractometer using a Cu Kα radiation source (0.1542 nm) at 40 kV and 150 mA. PL and PLE spectra are recorded by Jobin Yvon FL3-221-TCSPC fluorescence spectrophotometer with a 450 W xenon lamp as the excitation light source. Ultraviolet-visible absorption spectra is obtained by UV-4100 spectroscopy.

Typical XRD pattern and SEM image of the as-grown ZnO nanorods are shown in Fig.1. It can be seen that all diffraction peaks of the sample match well with the wurtzite ZnO crystal. The obtained ZnO nanorods with a hexagonal cross section are mainly 150 nm−200 nm in diameter and about 2 mm in length.

Fig.2(a) displays the typical ultraviolet-visible absorption spectra of ZnO nanorods annealed at 200 °C. The inset of Fig.2(a) shows plot of $(\alpha h\gamma)^2$ versus $h\gamma$, and we can calcu-

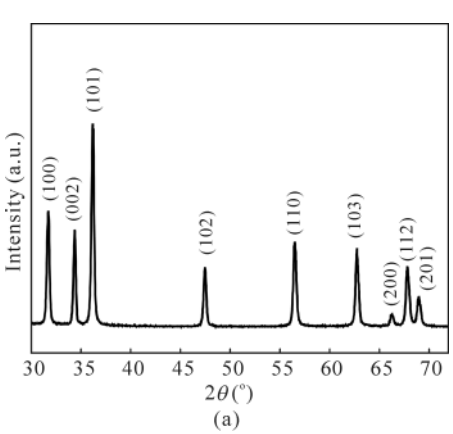

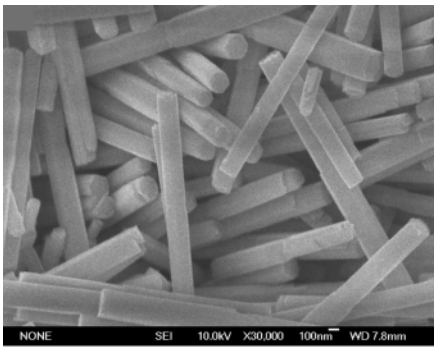

Fig.1(a) XRD pattern and (b) SEM image for the ZnO nanorods

late the direct band gap energy of 3.367 eV at 368 nm. PL spectra of ZnO nanorods annealed at different temperatures are shown in Fig.2(b). All samples exhibit a weak UV emission around 383 nm and a strong broad visible emission in 450 nm−700 nm region. As the annealing temperature increases, the UV emission and visible emission are both enhanced, and the ratio between UV emission and visible

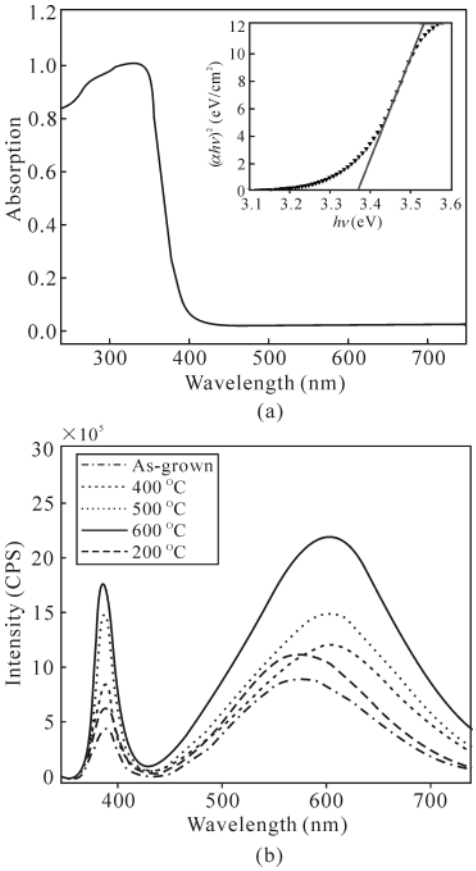

Fig.2(a) Ultraviolet-visible absorption spectrum of ZnO nanorods annealed at 200 °C in oxygen ambient; (b) PL spectra of as-grown and annealed ZnO nanorods in oxygen ambient at various temperatures (The excitation wavelength is 345 nm.)

emission is increased, which indicates the improvement of ZnO nanorods crystalline[18]. It is interesting that the visible emission is of red-shift characteristic with the annealing temperature increasing. In order to investigate the origin of the visible emission, the asymmetric broad visible emission for annealed ZnO nanorods can be deconvoluted into two subband emissions centered at 535 nm (green emission) and 611 nm (orange-red emission) by Gaussian-fitting analysis, as shown in Fig.3. It is obvious that the green emission decreases and the orange-red emission enhances for the samples annealed at the temperatures from 200 °C to 600 °C, resulting in the red-shift of the visible emission.

For ZnO nanorods prepared by the aqueous solution method at a low growth temperature, a large amount of defects[19-21] can be generated. After annealing in oxygen ambient, the intensities of the green emission and the orange-red emission have obvious change. In general, the green emission and orange-red emission for annealed ZnO nanorods are attributed to the defects of V_o and O_i, respectively[22-25]. During the thermal treatment in oxygen ambient, oxygen atoms can be diffused into the bulk, and they fill the oxygen vacancies or occupy the interstitial sites to form oxygen interstitials. As a result, the green emission related to V_o decreases and the orange-red emission related to O_i increases with the annealing temperature increasing, which is in agreement with the results of previous experimental and theoretical reports[22-26].

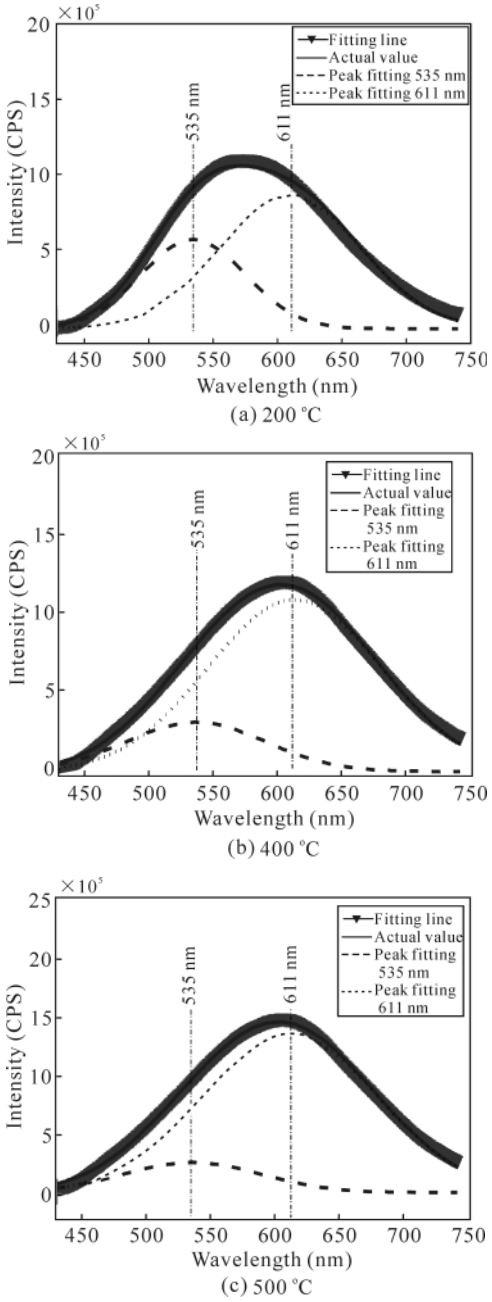

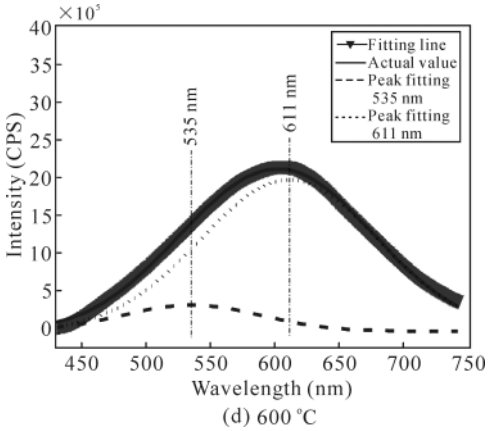

Fig.3 Gaussian-fitting analysis of the yellow-green emission annealed in oxygen ambient under different temperatures

To understand the features of the excited states related to the visible emissions, the PLE spectra of annealed ZnO nanorods are measured and the typical PLE spectra of sample annealed in 200 °C is presented in Fig.4(a) at different emission wavelengths. The peak at 372 nm is observed in all PLE spectra, which indicates that the preferential excitation energy is below the bandgap, and the initial state is located slightly below the conduction band-edge. Fig.4(b) exhibits the PL spectra of ZnO nanorods annealed in 200 °C at different excitation wavelengths. It can be observed that the peak position of the visible emission band has not changed at different wavelengths, but the intensity is decreased. The visible emission band also can be deconvoluted into green emission and orange-red emission by Gaussian-fitting analysis under the excitation wavelength at 372 nm and 385 nm, which is shown in Fig.4(c) and Fig.4(d).

According to the experimental and theoretical results[22-28], among all the possible native defects in ZnO lattice, only Zn_i is a shallow donor and the correspond erergy level is located slightly below the conduction band-edge at 0.22 eV[22,23], whereas V_o or O_i defects[27,28] can create deep levels above the valence band, but considerable controversy remains for the level positions. In this letter, a schematic diagram of the visible emission band related to defects is drawn in Fig.4(e).

Combining with the results of PLE and PL spectra at different excitation wavelengths for ZnO nanorods annealed in oxygen ambient, the visible emission bands can be attributed to Zn_i, V_o and O_i defects. At the different excitation wavelengths, the excited electrons can relax to Zn_i energy level and can be trapped by Zn_i defect centers, which induces effective transitions from Zn_i energy level to V_o or O_i deep levels. As shown in Fig.4(c) and Fig.4(d), the unvaried intensity ratio of green and orange-red emissions indicates that the numbers of recombined electron-hole (e-h) pair between Zn_i defect state and V_o or O_i defects state are the same under different excitation energies.

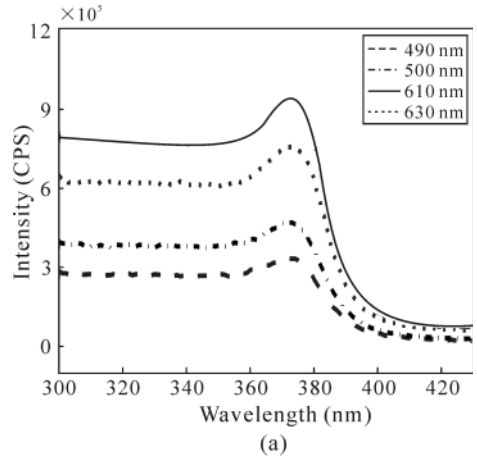

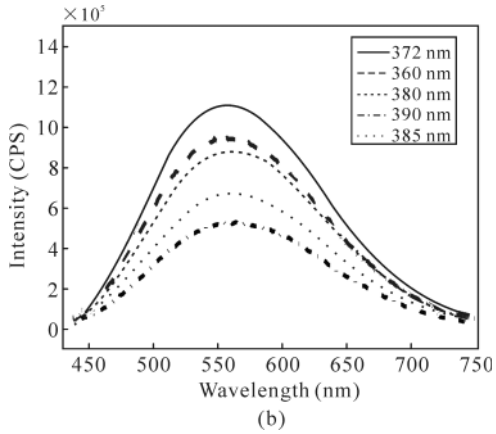

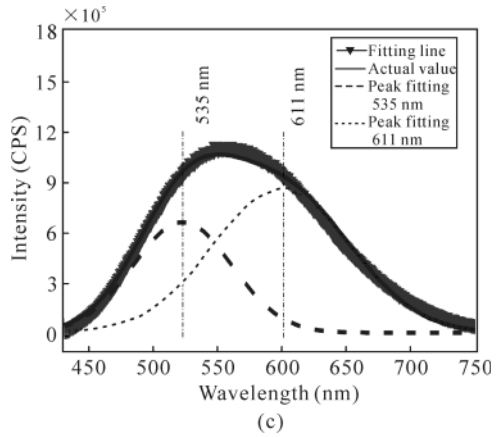

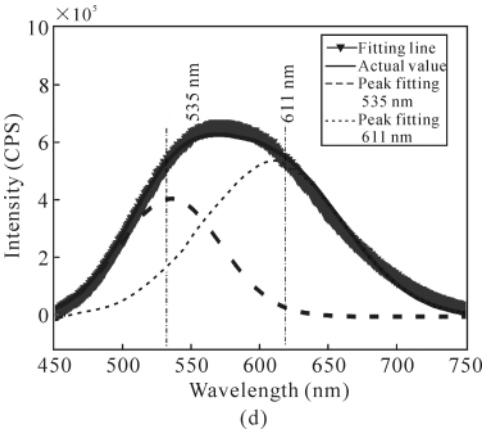

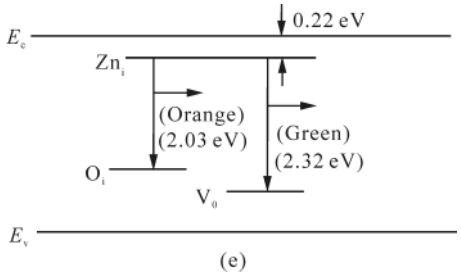

Fig.4(a) PLE spectra of the ZnO nanorods at different wavelengths; (b) PL spectra of ZnO nanorods excited by different wavelengths; (c) and (d) Gaussian-fitting spectra of the visible emission band in ZnO nanorods excited by wavelengths at of 372 nm and 385 nm, respectively; (e) Schematic diagram of band structures in the ZnO nanorods

In summary, we have investigated the visible emission properties of ZnO nanorods annealed in oxygen ambient at the temperature ranging from 200 °C to 600 °C. PL spectra of all annealed samples show a strong and broad visible emission band and can be Gaussian fitted into green emission and orange-red emission. PLE spectra and PL spectra at different excitation wavelengths reveal that the green and orange-red emissions are the radiative recombination of the trapped electrons in Zn_i defect erergy level with a deeply trapped hole in V_o defects and O_i defects, respectively.

References

[1] H. B. Zeng, X. J. Xu, Y. Bando, U. Gautam, T. Y. Zhai, X. S. Fang, B. D. Liu and D. Golberg, Adv. Funct. Mater. **19**, 3165 (2009).

[2] LI Xiang-ping, ZHANG Bao-lin, SHEN Ren-sheng, ZHANG Yuan-tao, DONG Xin and XIA Xiao-chuan, Journal of Optoelectronics • Laser **20**, 601 (2009). (in Chinese)

[3] J. Y. Zhuang, L. Li, X. S. Zhang, J. P. Xu and J. Wei, Optoelectronics Letters **5**, 1 (2009).

[4] Y. H. Yang, X. Y. Chen, Y. Feng and G. W. Yang, Nano Lett. **7**, 3879 (2007).

[5] N. W. Wang, Y. H. Yang and G. W. Yang, J. Phys. Chem. C

113, 15480 (2009).

[6] D. C. Look, G. C. Falow, Pakpoom Reunchan, Sukit Limpijumnong, S. B. Zhang and K. Nordlund, Phys. Rev. Lett. **95**, 225502 (2005).

[7] F. Tuomisto, V. Ranki and K. Saarinen, Phys. Rev. Lett. **91**, 205502 (2003).

[8] J. Y. Zhang, P. J. Li, H. Sun, X. Shen, T. S. Deng, K. T. Zhu, Q. F. Zhang and J. L. Wu, Appl. Phys. Lett. **93**, 021116 (2008).

[9] S. Lee, S. Jeong, D. Kim, B. Park and J. Moon, Superlattices Microstruct. **42**, 361 (2007).

[10] D. Q. Bi, F. Wu, W. J. Yue Y. Guo, W. Shen, R. X. Peng, H. Wu, X. K. Wang and M. T. Wang, J. Phys. Chem. C **114**, 13846 (2010).

[11] M. Quintana, T. Edvinsson, A. Hagfeldt and G. Boschloo, J. Phys. Chem. C **111**, 1035 (2007).

[12] M. W. Ahn, K. S. Park, J. H. Heo, J. G. Park, D. W. Kim, K. J. Choi, J. H. Lee and S. H. Hong, Appl. Phys. Lett. **93**, 263103 (2008).

[13] C. Y. Lee, J. Y. Wang, Y. Chou, C. L. Cheng, C. H. Chao, S. C. Shiu, S. C. Hung, J. J. Chao, M. Y. Liu, W. F. Su, Y. F. Chen and C. F. Lin, Nanotechnology **20**, 425202 (2009).

[14] X. Liu, X. Wu, H. Cao and R. P. H. Chang, J. Appl. Phys. **95**, 3141 (2004).

[15] A. B. Djurisic, W. C. H. Choy, V. A. L. Roy, Y. H. Leung, C. Y. Kwong, K. W. Cheah, T. K. Gundu Rao, W. K. Chan, H. Fei Lui and C. Surya, Adv. Funct. Mater. **14**, 856 (2004).

[16] N. Y. Garces, L. Wang, L. Bai, N. C. Giles, L. E. Halliburton and G. Cantwell, Appl. Phys. Lett. **81**, 622 (2002).

[17] A. B. Djurisic and Y. H. Leung, Small **2**, 944 (2006).

[18] S. H. Baek, J. J. Song and S. W. Lim, Physica B **399**, 101 (2007).

[19] D. Li, Y. H. Leung, A. B. Djurisic, Z. T. Liu, M. H. Xie, S. L. Shi, S. J. Xu and W. K. Chan, Appl. Phys. Lett. **85**, 1601 (2004).

[20] L. E. Greene, M. Law, J. Goldberger, F. Kim, J. Johnson, Y. F. Zhang, R. Saykally and P. D.Yang, Angew. Chem. Int. Ed. **42**, 3031 (2003).

[21] K. H. Tam, C. K. Cheung, Y. H. Leung, A. B. Djurišiæ, C. C. Ling, C. D. Beling, S. Fung, W. M. Kwok, W. K. Chan, D. L. Phillips, L. Ding and W. K. Ge, J. Phys. Chem. B **110**, 20865 (2006).

[22] E. G. Bylander, J. Appl. Phys. **49**, 1188 (1978).

[23] L. S. Vlasenko and G. D. Watkins, Phys. Rev. B **72**, 035203 (2005).

[24] H. F. Liu, S. J. Chua, G. X. Hu, H. Gong and N. Xiang, J. Appl. Phys. **102**, 043530 (2007).

[25] S. A. Studenikin, Nickolay Golego and Michael Cocivera, J. Appl. Phys. **84**, 2287 (1998).

[26] X. L. Wu, G. G. Siu, C. L. Fu and H. C. Ong, Appl. Phys. Lett. **78**, 16 (2001).

[27] S. B. Zhang, S. H. Wei and Alex Zunger, Phys. Rev. B **63**, 075205 (2001).

[28] B. Q. Cao, W. P. Cai and H. B. Zeng, Appl. Phys. Lett. **88**, 161101 (2006).